# INFLUENCE OF 3D PERTURBATIONS ON SEPARATED FLOWS

FRÉDÉRIC ALIZARD AND JEAN-CHRISTOPHE ROBINET
ENSAM CER de Paris - SINUMEF Laboratory, 151 boulevard de l'Hopital, 75013 Paris.
frederic.alizard@paris.ensam.fr, jean.christophe.robinet@paris.ensam.fr

**Abstract.** The origin of the onset of three dimensionality on a flat plate separated flow is discussed thanks to a parametric analysis from Falkner-Skan profiles. The study is aimed to illustrate the strong dependance of the bubble shape on the temporal growth rate and the centrifugal nature of the instability thanks to a comparison of the Rayleigh discriminant value and the global temporal growth rate.

**Key words:** global instability, separated flow, centrifugal nature.

## 1. Introduction.

Influence of three dimensional perturbations on separated flows has been studied in many configurations as well as on backward facing steps (experimentally by Beaudoin *et al.* [3] and numerically by Barkley *et al.* [1]) that on a flat plate (Theofilis *et al.* [7] and Wilson & Pauley [5]). However the 3D structure of the unstable separated flow seems to be very similar and quite independent of the geometry. Indeed the analysis realized by Barkley *et al.* [1] shows that the first intrinsic linear instability of the steady two-dimensional flow is a stationnary three-dimensional bifurcation whose the flat roll structure with a characteristic spanwise wavelength is very similar as the experimental visualization of Beaudoin *et al.* [3]. Moreover Wilson & Pauley [5] in their L.E.S study of a transitional separation bubble on flat plate identify the generation of stationary Goertler vortices in the spanwise direction and Theofilis *et al.* [7] thanks to a two dimensional linear stability analysis found that the most unstable eigenmode of a separated flow subjected to a 3D perturbation had an imaginary part equal to zero. All these results lead us to examine more precisely the influence of a 3D perturbation on a separated flow model and the nature of the instability. The paper is thus organized as follows. At first the basic flow is presented as well as the BiGlobal stability numerical method. Then the topological structure of the global unstable mode is presented. Finally a discussion on the instability mechanism and the nature of the instability is provided thanks to a parametric analysis.

## 2. Basic flow.

A family of Falkner Skan profiles was used to construct the separated flow (see Hammond & Redekopp [2]). In order to analyze more particularly the 3D transition phenomenon this kind of separated flows allows us to realize a parametric study.

$$f''' + ff'' + \gamma(1 - f'^2) = 0,\ f(0) = f'(0) = 0\ et\ f(\eta \to \infty) = 1, \qquad (1)$$

$$\begin{aligned} &\eta = y\sqrt{\frac{Re}{(2-\gamma)}x^{1-m}},\ \psi(x,y) = f\sqrt{\frac{(2-\gamma)x^{1-m}}{Re}}Ue, \\ &U(x,y) = \frac{\partial\psi}{\partial y},\ V(x,y) = -\frac{\partial\psi}{\partial x} \end{aligned} \tag{2}$$

with $U_e$ a dimensionless velocity $U/U_{ref} = x^m$, where $m = \gamma/(2-\gamma)$. A specific profile for the reduced pressure gradient $\gamma(x)$ provides a well defined separated flow on the flat plate (separation line is shown on figure 1).

## 3. BiGlobal stability numerical method.

### 3.1. General method.

The instantaneous flow is taken as $\mathbf{Q}(x,y,z,t) = \overline{\mathbf{Q}}(x,y) + \varepsilon\mathbf{q}(x,y,z,t) + cc,\ \ \varepsilon \ll 1$ where $\overline{\mathbf{Q}}$ is the steady two dimensional basic flow and $\mathbf{q}$ the perturbation which have the wave form: $\mathbf{q}(x,y,z,t) = \hat{\mathbf{q}}(x,y,z)e^{-i\Omega t}$ with $\hat{\mathbf{q}} = (\hat{u},\hat{v},\hat{w},\hat{p})^T$. Then the linearized 3D incompressible Navier-Stokes equations defined the following eigenvalue problem:

$$(\mathbf{u}.\nabla)\mathbf{U} + (\mathbf{U}.\nabla)\mathbf{u} - \nabla\hat{p} + \frac{1}{Re}\Delta\mathbf{u} - i\Omega\mathbf{u} = 0,\ \ \nabla.\mathbf{u} = 0 \tag{3}$$

with $\mathbf{u} = (\hat{u},\hat{v},\hat{w})^T$ and $\mathbf{U} = (U,V)^T$ and $i\Omega$ the eigenvalue. Direction $z$ is taken as homogeneous: $\hat{\mathbf{q}}(x,y,z) = \tilde{\mathbf{q}}(x,y)e^{i\beta z}$ with $\beta$ the spanwise wavenumber. Hereafter the system (3) is noted as :

$$\mathcal{L}\tilde{\mathbf{q}} \quad = 0 \tag{4}$$

### 3.2. Multi-Domain spectral collocation.

Considering global mode developping inside separated flow a multi-domain spectral collocation method is used to cluster points inside the bubble ([4]). The domain is decomposed into three domains I, II and III. The governing equations is thus written:

$$\mathcal{L}_{\mathrm{I}}\tilde{\mathbf{q}}_{\mathrm{I}} = 0,\ \mathcal{L}_{\mathrm{II}}\tilde{\mathbf{q}}_{\mathrm{II}} = 0,\ \mathcal{L}_{\mathrm{III}}\tilde{\mathbf{q}}_{\mathrm{III}} = 0 \tag{5}$$

where $\mathcal{L}_{\mathrm{I}}$, $\mathcal{L}_{\mathrm{II}}$ and $\mathcal{L}_{\mathrm{III}}$ denote operators and $\tilde{\mathbf{q}}_{\mathrm{I}}$, $\tilde{\mathbf{q}}_{\mathrm{II}}$ and $\tilde{\mathbf{q}}_{\mathrm{III}}$ eigenvectors defined in domain I, II and III respectively. A Chebyshev/Chebyshev collocation spectral method is used to discretize (5). Boundary conditions on domain I and III and interface conditions (6, 7) complete the system ($x_1$ and $x_2$ denoting interfaces position).

$$\tilde{\mathbf{q}}_{\mathrm{I}}|_{x=x_1} - \tilde{\mathbf{q}}_{\mathrm{II}}|_{x=x_1} = 0,\ \ \tilde{\mathbf{q}}_{\mathrm{II}}|_{x=x_2} - \tilde{\mathbf{q}}_{\mathrm{III}}|_{x=x_2} = 0 \tag{6}$$

$$\frac{d\tilde{\mathbf{q}}_{\mathrm{I}}}{dx}|_{x=x_1} - \frac{d\tilde{\mathbf{q}}_{\mathrm{II}}}{dx}|_{x=x_1} = 0,\ \ \frac{d\tilde{\mathbf{q}}_{\mathrm{II}}}{dx}|_{x=x_2} - \frac{d\tilde{\mathbf{q}}_{\mathrm{III}}}{dx}|_{x=x_2} = 0 \tag{7}$$

Finally the eigenvalue problem defined by system (5), (6) and (7) is solved thanks to a Shift and Invert Arnoldi algorithm.

## 4. Structure of the most unstable eigenmode and Multi-Domain performance.

Figure 1 illustrates the structure of the unstable global mode at Reynolds number $18000$ which is stationnary. The influence of the global mode is principally localized in the

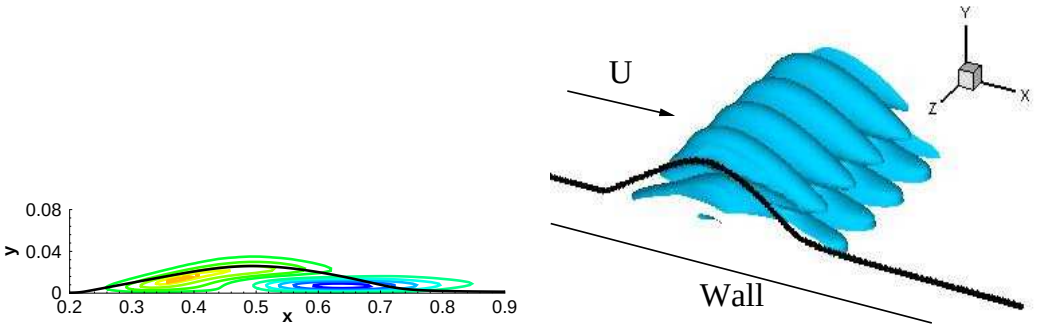


(a) Streamwise component of the perturbation. (b) 3D Iso-vorticity contours of the perturbation.

*Figure 1.* Perturbation obtained at Reynolds number equal to $30000$ and $\beta = 22$.

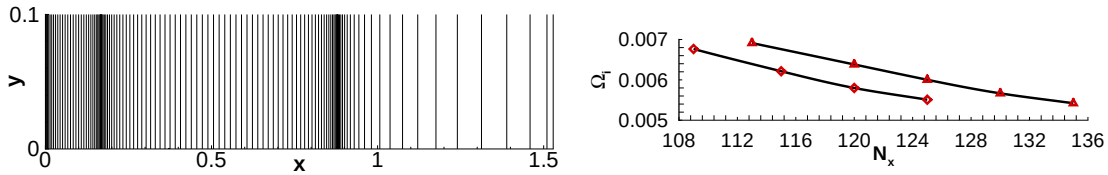


(a) (b)

*Figure 2.* (a) Grid used with $125$ points in the streamwise direction. (b) Temporal amplification rate evolution with $N_x$, the number of points in the streamwise direction for Reynolds number equal to $18000$. $50$ points is used in the normal direction. $\Delta$ characterizes the single-domain, $\diamond$ the multi-domain.

separated flow area. In order to improve the global mode's convergence, the grid on figure 2(a) is used for all calculation. A comparaison with single-domain is shown on figure 2(b).
From iso-vorticity contours of the disturbance on figure 1(b) the structure of the 3D perturbation takes the form of spanwise flat roll which appears around the separation line. This particular shape is caused by the transverse component of the perturbation (figure 1(a)) which injects fluid in each $z$ direction which is rolled up around the separation line. Furthermore it is interesting to see that perturbation (figure 1) follows the streamline's curvature. Consequently a parametric study on Reynolds number and on bubble shape is provided in the following parts to clarify the nature of this instability.

## 5. Discussions on the nature of the instability.

### 5.1. Influence of the Reynolds number, inviscid nature of the instability.

In order to study the inviscid nature of the instability, seven base flows are constructed thanks to Falkner-Skan profile with a same gradient pressure reduced imposed: Re $=$ $14000$, $18000$, $30000$, $40000$, $50000$, $60000$, $70000$ (which correspond to a $\mathrm{Re}_x = 0.05 \times$ Re). The neutral curve is represented on fig. 3(a). Temporal amplification rate levels $\Omega_i$ illustrate the global unstable area in a plane ($\beta$, Re), the transverse wave number and the Reynolds number respectively. Then the neutral curve shape is typical of an inviscid instability and more particularly a critical Reynolds number appears at $15000$.

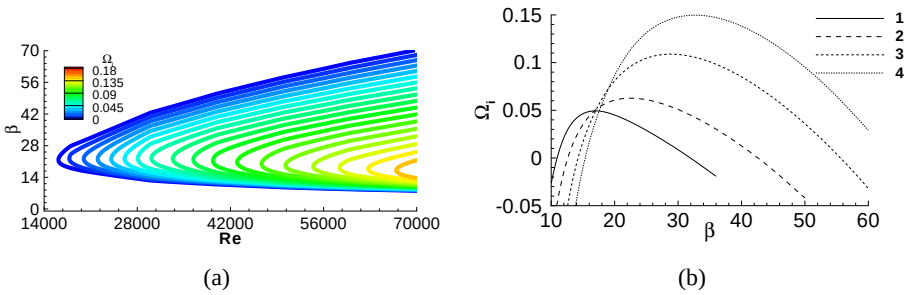


(a) (b)

*Figure 3.* (a) Neutral curve of the separated flow from the Falkner-Skan profiles. $\Omega_i$ represents the global temporal amplification rate. (b) Global temporal amplification rate $\Omega_i$ with the transverse wave number $\beta$ . Four bubble sizes are studied at Reynolds number: $30000$.

### 5.2. BUBBLE SHAPE ANALYSIS.

To analyse more particularly only the influence of the bubble shape on the instability the Reynolds number is fixed at Re $= 30000$ and a variation of separated zone is prescribed thanks to a change on the reduced pressure gradient profile without modifying the Falkner-Skan family (notably the reverse flow intensity). Four different profiles are used. Thereafter base flows $1$, $2$, $3$ and $4$ will denote separated flow of size: $0.588$, $0.525$, $0.45$ and $0.4$ respectively. Figure 3(b) shows the temporal amplification rate evolution of the perturbation with the transverse wave number for base flows $1$, $2$, $3$ and $4$. Then it is clear there is a strong influence of the temporal amplification rate with the shape of the separated zone. Furthermore more concentrated the vortex is and stronger the instability is.

### 5.3. INSTABILITY MECHANISM.

From the previous analysis it has been seen that a global intrinsic mode can be unstable in a separated flow model. Furthermore the inviscid nature and the strong dependance of the temporal growth rate with the bubble shape was illustrated. In particular the reduction of the bubble's size in keeping the same Falkner-Skan profiles allowed to increase the temporal amplification rate. However the global mode is an intrinsic phenomenon and consequently don't have to be excited continuously to exist. The Goertler nature of the instability can thus be excluded. Indeed as it refereed in the article [5], the Goertler instability is an extrinsic phenomenon of convective nature and consequently can not appear as globally unstable. Then a hypothesis can be argue on the nature of the instability. From the eigenfunction's transverse component the disturbance is principally localized in the separated flow and divides closed streamlines of the recirculation area into two zones where the perturbation exchanges fluid (figure 1). Moreover the steadiness of the disturbance allow the perturbation to always remain and amplify inside the closed streamlines. This kind of three dimensional phenomenon is a typical feature of centrifugal instability. A sufficient centrifugal condition based on a generalized Rayleigh criterion lead to an identification on unstable closed streamlines [6]:

$$\Delta(x) = 2\left(\frac{V(x)}{\varrho(x)}\right)\varpi(x) \tag{8}$$

with $x$ defining point of streamline considered, $\varrho$ is the local radius of curvature, $V$ the norm of the velocity and $\varpi$ the vorticity. The flow is unstable if there exist a closed

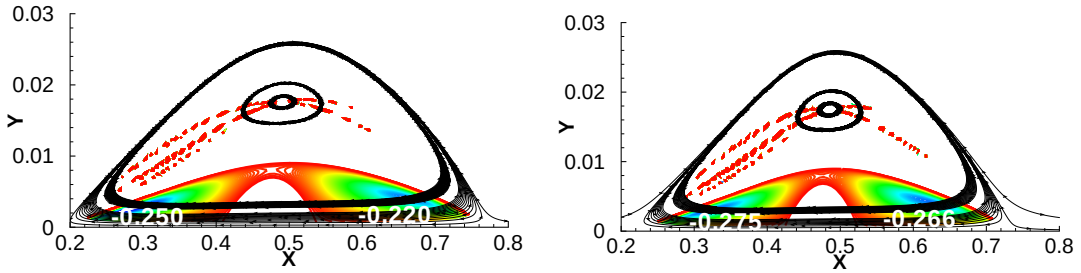


(a) Maximum temporal amplification rate: $\Omega_i = 0.0494$. (b) Maximum temporal amplification rate: $\Omega_i = 0.0627$.

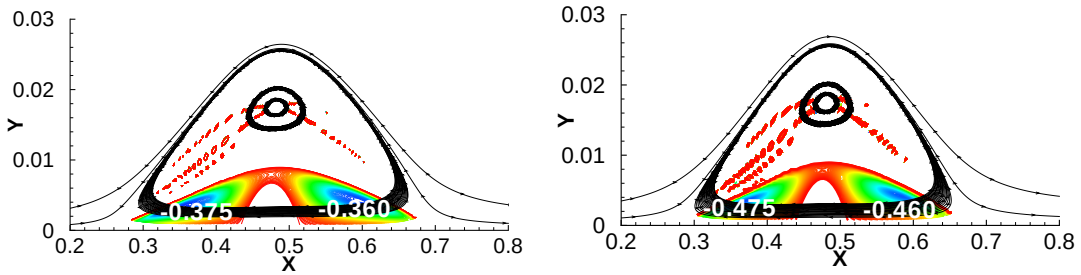


(c) Maximum temporal amplification rate: $\Omega_i = 0.1089$. (d) Maximum temporal amplification rate: $\Omega_i = 0.1497$.

*Figure 4.* Centrifugal zones where the relation (8) is negative inside closed streamlines. Reynolds number is 30000.

streamline $\varphi$ where:

$$\max_{\varphi}(\Delta(x)) \leq 0 \tag{9}$$

Consequently a similar study of the Rayleigh criterion's intensity as the Barkley *et al.* [1] confined backward facing step analysis is performed along closed streamlines for each bubble sizes. This analysis will aim to explain that closed streamlines shape inside bubble is a determining factor on the temporal amplification rate.

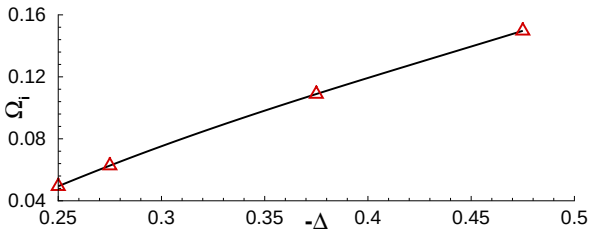


*Figure 5.* Evolution of temporal amplification rate $\Omega_i$ with the Rayleigh discriminant value (8) at Reynolds number equal to 30000.

From the figure 4 a study of the Rayleigh criterion evolution on the different bubble shape is performed. Even if the relation (9) is not verified on closed streamlines, fluid particles travel along streamlines into two large regions where (8) is negative. Otherwise the criterion (9) is only sufficient and the intensity of the relation (8) can allow to arise these instability. Furthermore from figures 4 it can be observed that Rayleigh discriminant intensity increases with the reduction of the bubble shape. Then fluid particles feel more the influence of the centrifugal instability which will be concordant with the fact the temporal amplification rate increases (figure 5).

## 6. Conclusions and perspective.

A parametric study of the onset of three-dimensional global stationary instability on a separated flow was studied. A similar three dimensional behavior as the Barkley stability

analysis [1] over a backward facing step was identify. Furthermore it was clearly illustrated the inviscid nature and the strong dependance on the temporal growth rate with streamlines shape. More particularly the evolution of the Rayleigh discriminant with the global growth rate seems to corroborate the centrifugal nature of the instability. A perspective can thus be expected on the competition between strong convective instabilities from the shear layer and this global mode, especially at higher Reynolds number.

## References

[1] Barkley D., Gomes M., and Genderson D.H. Three dimensional instability in flow over a backward-facing step. *J. Fluid. Mech*, 473:167–189, 2002.

[2] Hammond D.A. and Redekopp L.G. Local and global instability properties of separation bubbles. *Eur. J. Mech. B*, 17:145–164, 1998.

[3] Beaudoin J.-F., Cadot O., Aider J.-L., and Wesfreid J.E. Three-dimensional stationary flow over a backward-facing step. *Eur. J. Mech B/Fluids*, 23:147–155, 2004.

[4] M.R. Malik. On the stability of attachment-line boundary layers. *J. Comput. Phys.*, 86:376–413, 1990.

[5] Wilson P.G. and Pauley L. L. Two and three dimensional large-eddy simulations of a transitional separation bubble. *Physics of Fluids*, 10 (11):2932–2940, 1998.

[6] D. Sipp and L. Jacquin. Three dimensional centrifugal-type instabilities of two-dimensional flows in rotating systems. *Physics of Fluids*, 12 (7):1740–1748, 2000.

[7] Theofilis V., Hein S., and Dallmann U. On the origins of unsteadiness and three dimensionality in a laminar separation bubble. *Proc. R. Soc. London.*, 358:3229–3246, 2000.